Dissolution of lime into BOS slag: from laboratory experiment to industrial converter

Zushu Li[1),], Martyn Whitwood[1)], Stuart Millman[2)] and Johan van Boggelen[2)]*
1) Tata Steel RD&T, Swinden Technology Centre, Rotherham, United Kingdom
2) Tata Steel RD&T, Teesside Technology Centre, Middlesbrough, United Kingdom

Abstract: Fast dissolution of lime into slag is a key to form a suitable slag in the BOS process. Many studies have been carried out to investigate the dissolution of lime into slag regarding the mechanism, the dissolution rate (kinetics) and the effect of various factors such as the density, the particle size and the reactivity of the lime on the dissolution. The experiments reported were carried out either under static conditions by heating the slag/ lime mixture, dipping a lime rod into stagnant slag, directly observing the slag penetration into a lime rod by using X-ray, or under 'dynamic' conditions by rotating a lime rod in a synthetic slag, either of which may not be close to the conditions in the actual BOS process.

In this study, the dissolution of lime into BOS slag was studied by characterising lime particles in the slag samples taken from laboratory hot metal dephosphorisation experiments in an induction furnace, a 6t pilot plant converter and a 320t industrial converter. By comparing the lime dissolution behaviour into BOS slag under varying dynamic conditions in the present study with that under laboratory static experiments from literature, it is expected to provide more insights on the mechanism of lime dissolution into BOS slag in the BOS process.

Keywords: Lime, Dissolution, Mechanism, BOS slag

1. Introduction

In the basic oxygen steelmaking (BOS) process, effective control of slag formation can provide a great opportunity to increase the process productivity, to improve the steel quality produced and to reduce the production cost. Lime dissolution is directly related to the slag formation behaviour in the BOS process. Fast dissolution of lime into slag is considered to be a key for the formation of a suitable slag in the BOS process. Therefore, much attention has been paid to investigate the dissolution of lime into the slag relating to BOS process (BOS slag). The studies on the dissolution of lime (including dolomite) into slag reported in the literature have the following features:

(1) Factors affecting the dissolution of lime into slag in relation to kinetics (rate), mechanism, etc. have been investigated such as the density of lime [1], the particle size [2, 3] and the reactivity of lime [2, 4].

(2) Synthetic slags such as 'FeO'-SiO_2, CaO-'FeO'-SiO_2 and CaO-SiO_2-'FeO'-P_2O_5 slags were used simulating the slags in various periods of the BOS process [4].

(3) The experiments were carried out either under static conditions by heating the slag / lime mixture [4], dipping a lime rod into the (stagnant) slag [2, 4], direct X-ray observation of the slag penetration into a lime rod [5], or through so-called 'dynamic' experiments by rotating a lime rod in a synthetic slag [6, 7, 8], either of which may not be close to conditions in the actual BOS process.

(4) It is generally concluded that a dense di-calcium silicate layer or a di-calcium silicate-calcium phosphate (C_2S-C_3P) layer for the phosphors-containing slag (depending on the FeO content in the slag) was found close to the surface of lime which retards the further dissolution of lime into slag for the static experiments [9] .

(5) Based on the formation of a C_2S layer surrounding the lime particles and the fact that phosphorus is mainly concentrated in the C_2S phase as a C_2S-C_3P solid solution [10, 11], it is also suggested that adding fine lime particles in the end period of converter blowing can promote the phosphorus refining by forming a C_2S-C_3P solid solution on the lime particle surface.

In this study, the lime dissolution behaviour into BOS slag was investigated by characterising the lime particle and its surrounding area in the slag samples taken from laboratory hot metal dephosphorisation experiments in an induction furnace, a 6t pilot plant converter and a 320t industrial converter. By comparing the lime dissolution behaviour into BOS slags under varying dynamic conditions in the present study with that under laboratory static experiments from literature, it is expected to provide more insights into the mechanism of lime dissolution into BOS slags under varying conditions and in the BOS process.

2. Slag sample from laboratory hot metal dephosphorisation experiment

2.1 Hot metal dephosphorisation experiment in an induction furnace

An induction furnace (200 mm inner diameter, capacity 80 kg, MgO-based refractory) was used to carry out hot metal dephosphorisation experiments with a mixture of lime and iron ore fluxes. 40 kg pig iron (3.78% C, 0.24% Si, 0.26% Mn and 0.142% P) was melted and maintained at 1400±20°C. Then the dephosphorisation of hot metal was performed by adding a batch of 67.0 g lime and 232.4 g iron ore mixture onto the hot metal every two minutes. In total ten batches were added.. The iron ore used contains 66.42% TFe, 3.30% SiO_2, 0.93% Al_2O_3, 0.02% MnO and 0.049% P. Feeding iron ore onto the hot metal was designed to provide oxygen to oxidise C, Si, Mn, P, S etc in the hot metal simulating oxygen blowing in the BOS process. The amount of iron ore added was calculated by considering the oxidation of carbon (partially), silicon, manganese (partially) and phosphorus in the hot metal. The amount of lime used was to aim at a slag basicity of $\%CaO/\%SiO_2$=2.0. Both lime and iron ore were crushed into <1 mm particles and mixed prior to use. Slag samples were taken at desired times to investigate the dissolution behaviour of lime into the slag.

2.2 Dissolution of lime into slag in the hot metal dephosphorisation experiment

Slag samples were taken from the hot metal dephosphorisation experiments at desired timings and naturally cooled. They were cold-mounted with Epoxy resin, polished, and observed for lime particles using a Philips XL40 SEM and composition analysis using the associated EDA facility. The same procedures for the sample preparation and observation were also applied to the slag samples taken from a 6t pilot plant converter and a 320t industrial converter.

Lime particles were observed in the slag sample taken at 2 minutes after adding fluxes onto the hot metal. Figure 1 shows the backscattered electron (BSE) image of a lime particle surrounded by slag and element mapping for part of the lime particle. As shown in Figure 1, the slag was found to penetrate into the lime along the cracks / pores in the lime,

which is considered as one of the major steps in the course of lime dissolution into slag [2, 11]. The variation of chemical composition across the slag-lime boundary was shown in Table 1. Two layers that have a big difference in chemical composition from either slag or lime were detected surrounding the lime particle: a very thin layer containing 6.0% P_2O_5 next to the slag and a relatively thick FeO/MnO-rich layer next to the lime. The former is labelled here as a C_2S-C_3P solid solution layer since the molar ratio of CaO, SiO_2 and P_2O_5 in this layer is close to the composition of C_2S-C_3P. The FeO/MnO detected in the C_2S-C_3P layer might be reflected from the adjacent FeO/MnO-rich layer or slag layer because the C_2S-C_3P layer was very thin. The P_2O_5 content in the C_2S-C_3P layer was much higher than that in the slag (1.22%), FeO/MnO-rich layer (0.40%) and lime (0.0%). The SiO_2 content in the FeO/MnO-rich layer was much lower than that in the slag. It should be noted that no tri-calcium silicate (C_3S) layer was detected.

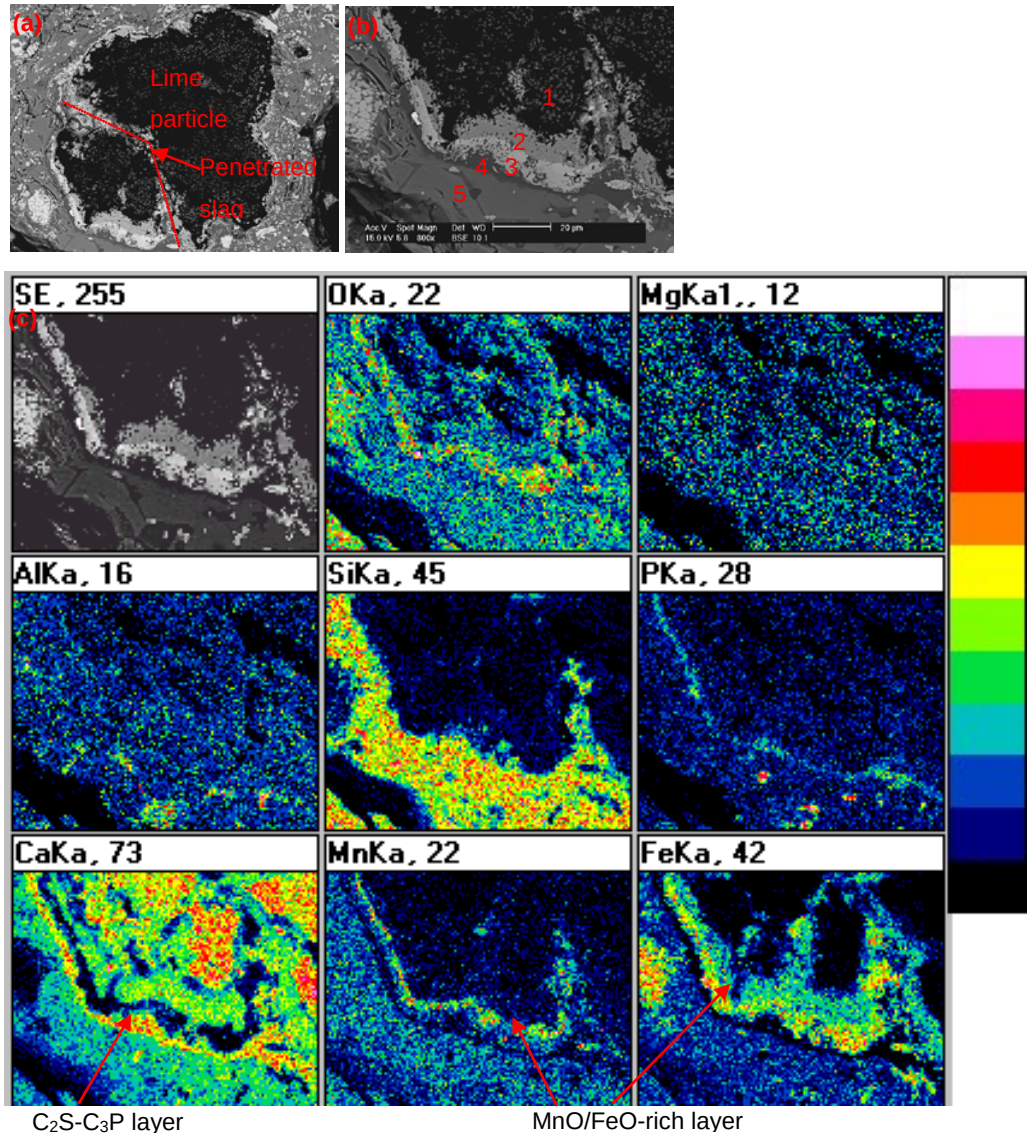

Fig. 1 (a) & (b) BSE image and (c) element mapping for the slag sample taken at 2 minutes from the start of the experiment showing the dissolution of a lime particle.

Table 1: Chemical composition across the slag-lime boundary as shown in Figure1b

Point in Figure1b	1	2	3	4	5
CaO	92.98	43.45	18.96	55.27	28.44
SiO_2	-	1.78	8.05	27.10	31.12
FeO	2.98	48.93	49.79	7.55	24.09
MnO	2.88	3.68	21.2	2.96	13.84
MgO	0.67	-	1.16	0.27	0.86
P_2O_5	-	-	0.42	6.07	1.22
Note	Lime	FeO/MnO-rich layer		C_2S-C_3P layer	Slag

Figure 2 shows another example of the lime dissolution into the slag which was taken at 10 minutes after the start of the experiment. A lime-Fe_xO cluster with a size of ~700 μm was found in the slag sample as shown in Figure 2a. The core of the lime-Fe_xO cluster can be considered as reacted lime and iron ore particles (Figure 2b) as it is evidenced by the composition in Figure 2b of point 1 for lime (92.5% CaO, 7.0% FeO and 0.5% MgO) and point 2 for iron ore (50.6%FeO, 45.4%CaO, 2.9%Al_2O_3 and 1.2% SiO_2) while MnO was not detected in the area. As shown in Figure 2c, the lime-Fe_xO cluster was surrounded by a relatively thick (up to ~50 μm) layer containing a significant amount of phosphorus (Table 2). EDA analysis shows this layer is similar to the composition of the solid solution C_2S-C_3P. The C_2S-C_3P layer can be further divided into two sub-layers: the sublayer next to lime is a layer of small C_2S-C_3P grains with FeO/MnO accumulating in the boundaries while the sublayer next to slag is pure C_2S-C_3P. Next to the C_2S-C_3P layer was a layer with much higher FeO and MnO contents than in the slag. It should be noted that the FeO/MnO-rich layer in Figures 1 and 2 contained high levels of MgO and low levels of CaO.

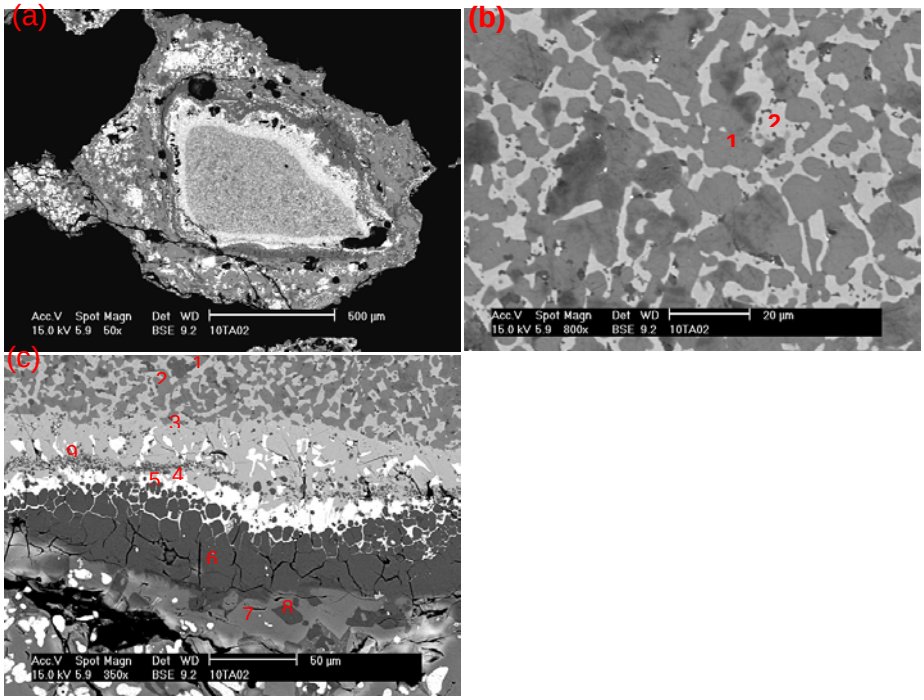

Fig. 2 (a) Image of the lime-Fe_xO cluster in the slag taken at 10 minutes after the start of the experiment, (b) image of the centre of the lime-Fe_xO cluster and (c) image of the slag-lime / Fe_xO cluster interface showing the C_2S-C_3P layer.

Table 2: Change in chemical compositions (%) across the slag-lime interface

Figure	Point	CaO	SiO_2	P_2O_5	MnO	FeO	MgO	Al_2O_3	Note
2(b)	1	92.5	-	-	-	7.0	0.5	-	Lime
	2	45.4	1.2	-	-	50.6	-	2.9	CaO-FeO
2(c)	1	52.7	0.9	-	-	44.4	0.2	1.8	CaO-FeO
	2	91.7	-	-	1.6	6.0	0.7	-	Lime
	3	44.9	1.5	-	1.5	48.3	-	2.6	CaO-FeO
	4	3.1	-	-	13.4	81.3	2.2	-	FeO/MnO-rich layer
	5	62.8	29.9	5.9	-	1.4	-	-	C_2S-C_3P
	6	62.2	30.2	6.7	-	0.7	-	-	C_2S-C_3P
	7	33.5	32.3	1.2	5.4	24.4	3.3	-	Slag
	8	55.4	12.5	29.3	1.1	1.7	0.2	-	C_2S-C_3P
	9	64.0	30.5	3.0	-	2.2	-	0.4	C_2S-C_3P

3. Slag sample from six-ton pilot plant converter

Trials in a six-ton pilot plant converter were carried out to improve phosphorus refining performance in the BOS process [12, 13]. Slag / metal emulsion samples were taken at seven specified positions in the converter simultaneously. This was repeated eight times during the blow using a new automated sampling system. Figure 3(a) shows a lime particle in the slag sample taken at 2 minutes after the oxygen blowing was started.

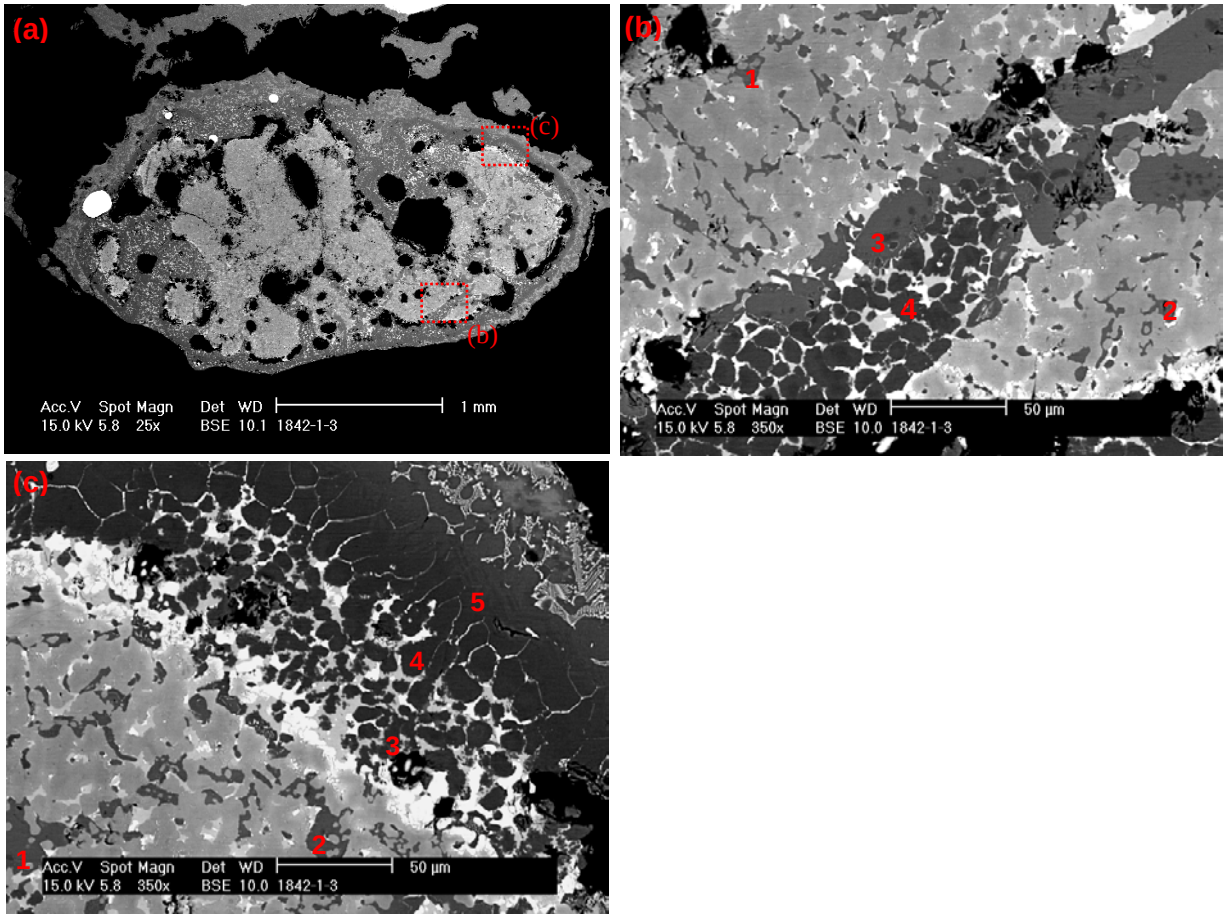

Fig. 3 (a) A lime particle in the slag taken from the 6-ton pilot plant converter at 2 minutes from the start of the blow; (b) Penetration of the slag along large channels and small capillaries in the lime. 1, 2 & 3: C_3S; 4-C_2S; (c) The morphology of lime particle-slag interface. 1&2: C_3S; 3 to 5: C_2S surrounded by the FeO/MnO-rich slag.

It can be seen from Figure 3(a) that the lime particle was penetrated by the slag in three-dimensions along large channels (cracks or pores) as well as small capillaries. This behaviour is further characterised in Figure 3(b). The chemical composition of typical phases in Figure 3(b) was listed in Table 3. It was found that:

- The substance which filled the capillaries in the lime particle was tri-calcium silicate with 0.5~0.7% P and high FeO-containing materials (points 1 and 2 in Figure 3(b));
- There was a layer of tri-calcium silicate along the large channels (in dark grey, e.g. point 3 in Figure 3(b));
- Next to the tri-calcium silicate layer in the large channel are di-calcium silicate grains surrounded by high-FeO materials.

The lime-slag interface was also characterised as shown in Figure 3(c) with the chemical composition in Table 3. It was found that:

- The substance that filled the capillaries in the lime particle was tri-calcium silicate with 0.5~0.7% P and high FeO-containing materials (points 1 & 2 in Figure 3(c));
- At the lime-slag interface, the layer next to lime is the FeO-MnO-CaO layer (in white);

Next to the FeO-MnO-CaO layer is a layer with di-calcium silicate grains surrounded by high-FeO materials. The size of the grains increased when the position is away from the lime particle. However, unlike that observed in Figure 2(c), no pure C_2S(-C_3P) layer was observed in Figure 3.

Table 3 Change in chemical compositions (%) across the slag-lime interface

Figure	Point	CaO	SiO_2	P_2O_5	MnO	FeO	MgO	Al_2O_3	Note
3(b)	1	67.2	24.2	0.5	0.9	4.8	0.5	1.6	C_3S
	2	69.0	24.8	0.6	1.5	2.9	-	-	C_3S
	3	68.6	24.8	0.5	1.3	3.0	0.3	-	C_3S
	4	63.2	32.0	1.4	-	0.9	-	-	C_2S
3(c)	1	69.1	24.9	0.6	1.2	2.9	-	-	C_3S
	2	69.7	23.4	0.4	1.6	3.3	-	-	C_3S
	3	65.0	31.7	0.8	-	1.8	-	-	C_2S
	4	62.5	31.5	0.8	0.4	1.0	-	-	C_2S
	5	61.5	33.0	1.9	1.1	0.8	-	-	C_2S

Another typical example of lime dissolution into the slag is shown in Figure 4. This slag sample was also taken from the same heat of the six-ton pilot plant converter trial at 2 minutes from the start of blow. The chemical composition of the points showing in the Figure 4(b) is listed in Table 4. In comparison with the behaviour shown in Figure 2, no C_2S-C_3P layer was found surrounding the fine lime particles. The edge of the fine lime particles was an FeO/MnO-rich layer. Tri-calcium silicate (C_3S) is also observed in the centre of lime particles (e.g. point 1 in Figure 4(b)).

Table 4: Change in chemical compositions (%) across the slag-lime interface (Figure 4(b))

point	CaO	SiO_2	P_2O_5	MnO	FeO	MgO	Al_2O_3	TiO_2	V_2O_5	Note
1	69.3	24.5	-	1.2	2.5	0.4	-	0.6	1.6	C_3S
2	88.2	-	-	3.9	6.9	0.9	-	-	-	CaO
3	17.1	0.7	-	20.0	55.6	3.1	0.5	0.2	1.8	FeO/MnO-rich
4	61.8	29.9	1.4	0.6	2.8	-	-	0.5	3.1	C_2S-C_3P

5	60.6	31.7	1.5	1.5	1.7	0.3	-	-	2.7	C_2S-C_3P
6	36.0	27.7	1.3	7.8	18.7	0.8	0.7	1.2	6.0	slag

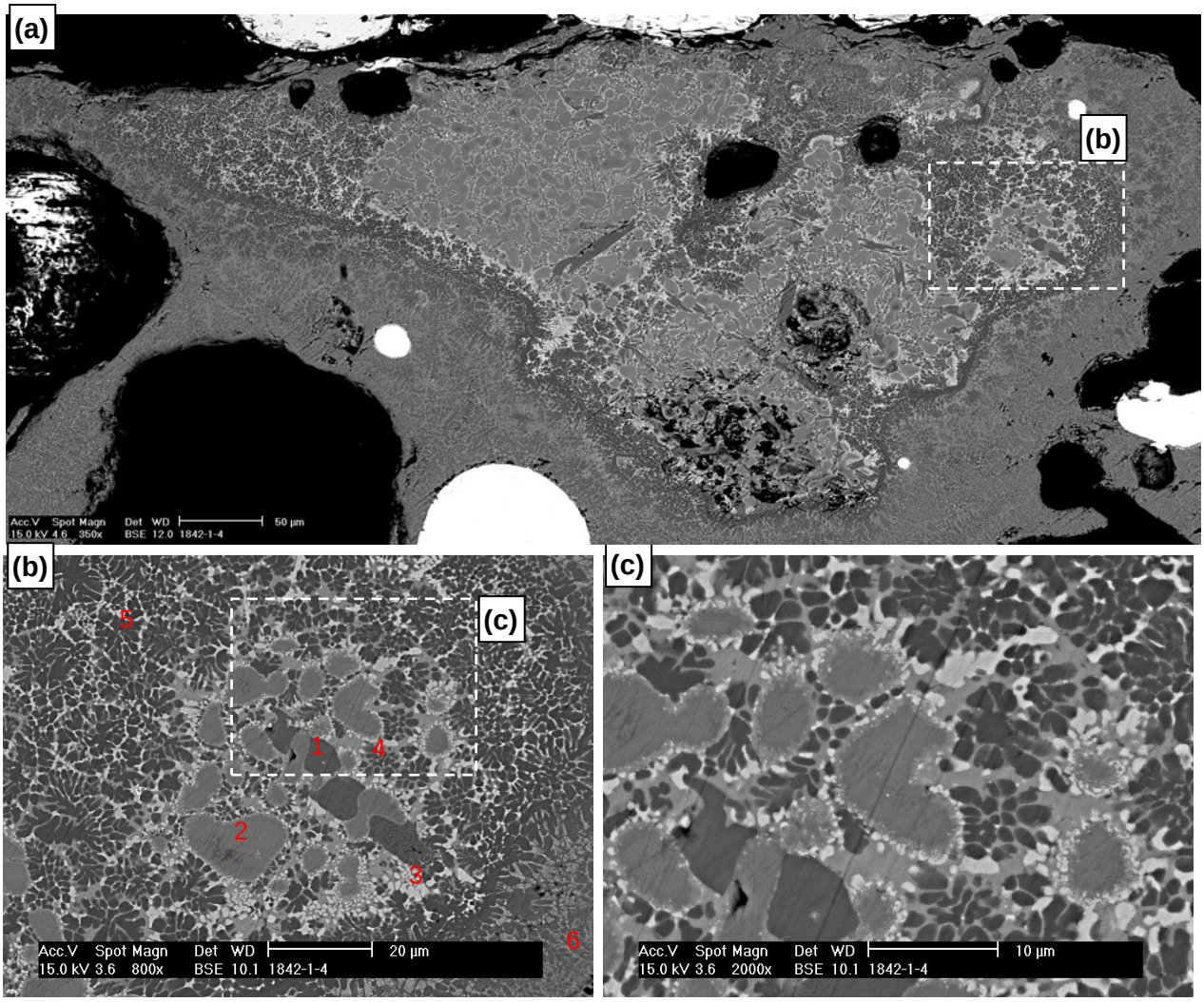

Fig. 4 (a) A lime particle in the slag taken from the 6-ton pilot plant converter at 2 min from the start of the blow; (b) & (c) The morphology of lime-slag interface.

4. Slag sample from 320t industrial converter

BOS slag samples were taken from a 320 ton converter during vessel tapping using a chain attached to the tip of the slag dart machine. A typical image and element mapping of the BOS slag are shown in Figure 5, and EDA results for different positions in Figure 5 are shown in Table 5. For this particular heat, excess amount of lime was added during the blow than was predicted by the charge balance model. This BOS slag did provide the opportunity to investigate the dissolution behaviour of lime in the BOS slag.

As shown in Figure 5 and Table 5, the BOS slag mainly consists of free lime (the lime particle with 83.2% CaO), Fe-rich monoxide, (both Fe- & Ca-rich) monoxide, tri-calcium silicate (C_3S), di-calcium silicate-calcium phosphate solid

solution (C_2S-C_3P), etc. Phosphorus was concentrated in both a C_2S-C_3P solid solution (≥ 5.1% P_2O_5) and C_3S (2.2% P_2O_5). The slag is laminated C_3S, C_2S-C_3P and monoxide. The C_2S-C_3P layer is thinner than the C_3S layer. Between the C_2S-C_3P layer and the C_3S layer there is always a monoxide layer (white line in Figure 5). Unlike the observations in the slags taken from laboratory lime dissolution experiments (Figures 1 and 2), no dense and continuous C_2S-C_3P layer was observed surrounding the lime particles.

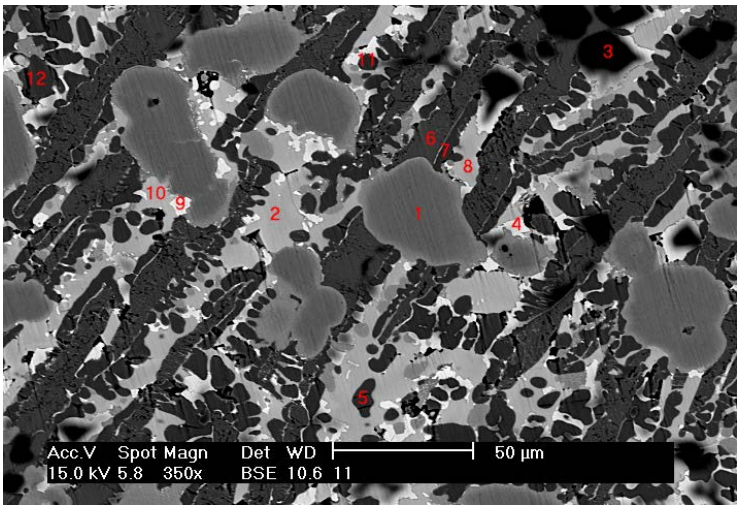

Fig. 5 Microstructure of the BOS slag taken from a 320t industrial converter.

Table 5 EDA results for BOS slag taken from a 320 t industrial converter

Point	Composition (wt.%)									Phase
	MgO	Al_2O_3	SiO_2	P_2O_5	S	CaO	TiO_2	MnO	FeO	
Area	5.0	0.4	12.0	1.7	0.1	56.5	0.7	5.0	18.7	
1	4.4	0.0	0.0	0.0	0.0	83.2	0.0	6.6	5.9	Free lime
2	0.6	1.7	2.2	0.0	0.0	45.2	5.6	1.7	43.1	Monoxide
3	70.6	0.0	0.0	0.0	0.0	3.0	0.0	7.7	18.6	MgO-rich monoxide
4	11.6	0.0	0.0	0.0	0.0	9.1	0.0	15.8	63.5	FeO-rich monoxide
5	0.0	0.3	28.3	5.1	0.0	63.4	0.7	0.0	2.2	C_2S-C_3P solid solution
6	0.0	0.0	24.2	2.2	0.0	69.8	0.0	1.0	2.8	Tri-calcium silicate
7	0.0	0.4	27.0	6.7	0.0	62.9	0.8	0.0	2.2	C_2S-C_3P solid solution
8	0.5	2.2	2.7	0.0	0.0	45.6	6.3	1.5	41.2	Monoxide
9	4.4	0.0	0.0	0.0	0.0	17.8	0.0	16.6	61.3	FeO-rich monoxide
10	0.2	2.4	1.5	0.0	0.0	45.7	1.6	1.0	47.6	Monoxide
11	0.0	0.3	27.8	6.1	0.0	62.9	0.8	0.0	2.0	C_2S-C_3P solid solution
12	0.0	0.2	27.1	6.7	0.0	62.7	0.9	0.0	2.4	C_2S-C_3P solid solution

Since the major interest is to characterise the lime particle and its surrounding area, more detailed observation has been done for a lime particle and its surrounding area, as shown in Figure 6 and Table 6.

The results from Figure 6 and Table 6 showed that:

- There is a clear gradient of Fe, Mn and Mg concentrations from the edge to the centre of lime particle. As shown in Figure 6(b), from the edge (point 1) to the centre (point 7), the concentrations of Fe, Mn and Mg decrease while the Ca content increases. This evidences that lime dissolution is led by the fast inward diffusion of Mn^{2+}, Fe^{2+} and Mg^{2+} ions. This also implies that the lime particle in this slag is undissolved lime.
- No continuous C_2S-C_3P layer (thin or thick) was observed surrounding the lime particle.

- The C_2S-C_3P phase was connected to the C_3S phase via a Fe/Mn-rich monoxide layer.

Table 6: EDA Results of a lime particle and its surroundings for BOS slag (Figure 6(b))

Position	Composition wt.%								Phase
	MgO	Al_2O_3	SiO_2	P_2O_5	CaO	TiO_2	MnO	FeO	
7	4.5	0.0	0.0	0.0	83.6	0.0	6.2	5.7	Free lime
6	4.3	0.0	0.0	0.0	83.4	0.0	6.5	5.9	Free lime
5	4.6	0.0	0.0	0.0	83.0	0.0	6.5	5.9	Free lime
4	3.8	0.0	0.0	0.0	80.7	0.0	7.3	8.1	Free lime
3	3.6	0.0	0.0	0.0	74.8	0.0	8.8	12.8	Free lime
2	3.0	0.0	0.0	0.0	67.7	0.0	10.7	18.6	CaO-rich monoxide
1	1.7	0.0	0.0	0.0	66.7	0.0	10.1	21.5	CaO-rich monoxide

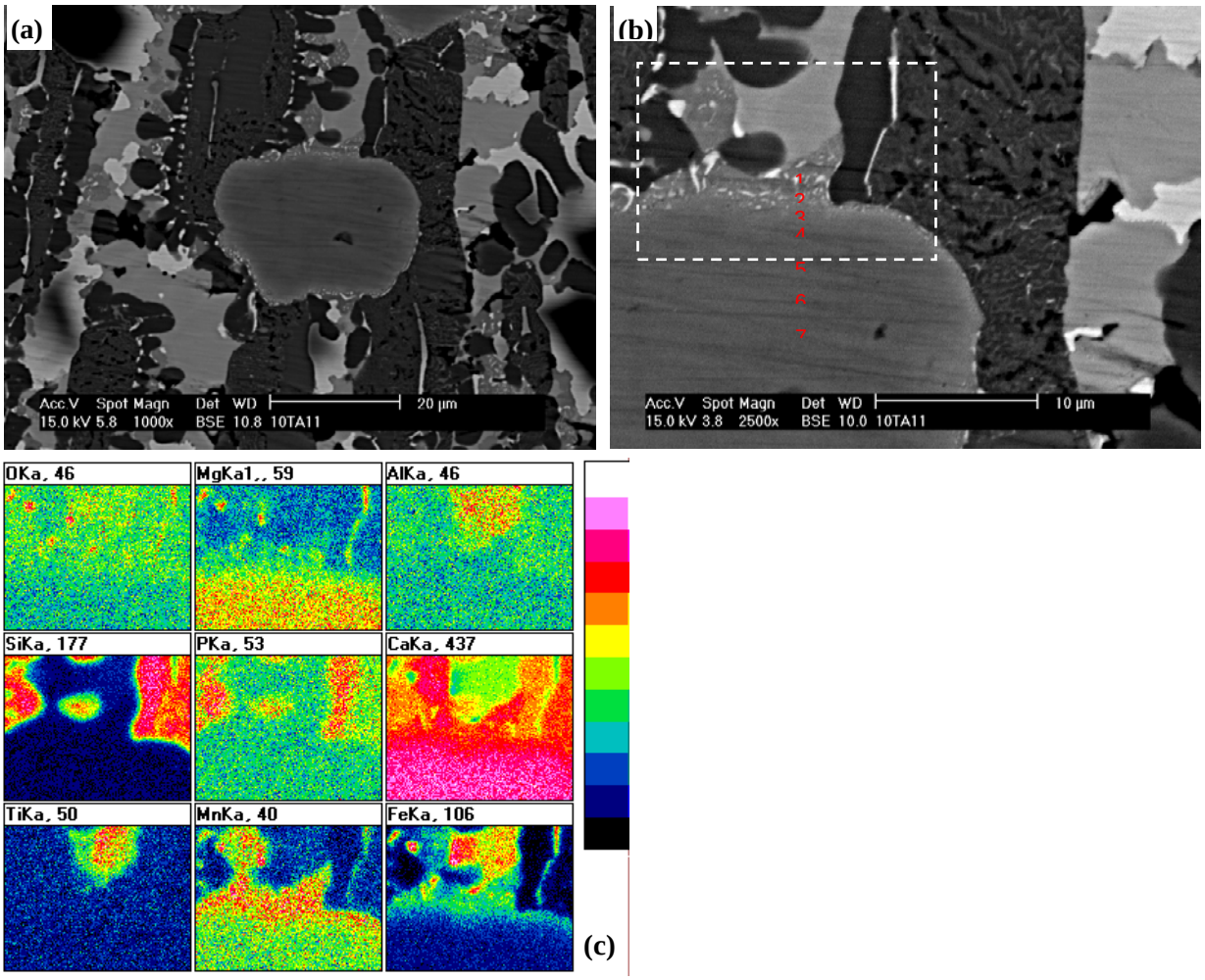

Fig. 6 Image and element mapping of a lime particle and surroundings in the BOS slag taken from the 320t industrial converter.

5. Discussion

As clearly shown in Figures 1 and 2 and Tables 1 and 2, two layers between the lime particle and slag were detected: an FeO/MnO-rich layer (also containing high MgO and low CaO contents) next to the lime and a C_2S-C_3P layer next to

the slag, which is similar to that reported in literature [4, 6, 10, 11]. However, unlike the findings in literature [4, 6, 10, 11], no tri-calcium silicate ($3CaO{\cdot}SiO_2$) was detected at the lime-slag interface in the slag sample taken from laboratory hot metal dephosphorisation experiment. It should be noted that in the present study the kinetic condition in the laboratory hot metal dephosphorisation experiment can be considered much more dynamic than that in laboratory experiments under static conditions [4, 6, 10, 11] due to the electric induction stirring and slag foaming. Two typical cases of lime dissolution into slag, as shown in Figure 3(c) and Figure 4(b) respectively, were observed in the slag sample taken from the 6t pilot plant converter. The first example in Figure 3(c) showed a similar lime-slag interface to that observed in Figures 1&2, i.e. an FeO/MnO-rich layer next to the lime and a C_2S layer next to the slag. However, this C_2S layer is not a dense and continuous C_2S layer but a layer of C_2S grains with high FeO/MnO accumulating on the grain boundaries. For the second example in Figure 4(b), although the edge of lime particles is rich in FeO and MnO, there is no clear C_2S layer surrounding the lime particles. For the slag sample taken from the 320t industrial converter, no continuous C_2S layer was observed surrounding the lime particles while obvious gradients of Fe and Mn were observed from the edge to the centre of lime particle (Figure 6b and Table 6).

Based on the fact observed in the slag samples as described above, the dissolution of lime can be considered to be caused by two-direction diffusion, i.e. inward diffusion of slag components into lime and outward diffusion of lime into slag. The inward diffusion is led by the faster diffusion of Fe^{2+}, Mn^{2+} and Mg^{2+} ions resulting in the formation of a FeO/MnO/MgO-rich layer, followed by the diffusion of anion complexes such as SiO_4^{4-} and PO_4^{3-} resulting in the formation of a C_2S-C_3P layer in the region where Ca^{2+}, SiO_4^{4-} and PO_4^{3-} is in the right ratio. This is probably attributed to the fact that the radii of Fe^{2+}, Mn^{2+} and Mg^{2+} ions are much smaller than those of the anion complexes SiO_4^{4-} and PO_4^{3-}. The radii of Fe^{2+}, Mn^{2+} and Mg^{2+} ions are 0.78, 0.80 and 0.72 Å respectively while the radii of SiO_4^{4-} and PO_4^{3-} are 2.79 and 2.76 Å. Another possible reason for the formation of a high FeO/MnO layer observed in the slag samples is, when the di-calcium silicate layer formed, the other components in this layer (except P_2O_5) have been pushed away from this layer. This is evident from the fact shown in Figure 2 and Figure 3(c) that the precipitated C_2S crystals are surrounded by the high Fe/Mn slag at the edges.

The effect of Fe^{2+} on lime dissolution has been studied in the literature (e.g. [2, 14]) while not much is reported on the effect of Mn^{2+} and Mg^{2+}. Mn^{2+} and Mg^{2+} ions due to their smaller radii diffuse faster than the anion complexes SiO_4^{4-} and PO_4^{3-} as described above. Furthermore Mn^{2+} and Mg^{2+} ions can break the Si-O and P-O networks and subsequently reduce the viscosity of the liquid slag. The penetration of molten slag into the lime cracks / pores or capillaries can be explained by the capillary force. Under this theory the depth penetrated by the molten slag increases with decreasing viscosity of the molten slag. Therefore, Fe^{2+}/Mn^{2+}/Mg^{2+}-containing slag due to its lower viscosity can penetrate more easily into the cracks / pores and capillaries of the lime speeding its dissolution into slag.

At the same time, Ca^{2+} diffuses in the opposite direction of the diffusion of Fe^{2+}, Mn^{2+} and Mg^{2+} ions, i.e. from lime into the slag, as evidenced by the gradient of CaO content from lime to slag shown in Tables 1 and 2. In the region where the outward Ca^{2+} and the inward SiO_4^{4-} are in the right molar ratio, a C_2S phase can be formed. The existence of P_2O_5 is likely to increase the possibility of the C_2S formation from the view point of thermodynamics ($2CaO{\cdot}SiO_2$-$3CaO{\cdot}P_2O_5$ phase diagram) [15]. This C_2S layer may be solid under experimental conditions (temperature, slag composition etc.) and can also be a precipitated product during the cooling of the sample as shown in Figure 2 and Figure 3 in the sublayer of C_2S-C_3P next to lime. In this C_2S-C_3P sublayer, the C_2S-C_3P phase precipitated with FeO/MnO accumulating in the boundaries.

The C_2S-C_3P layer is generally observed at the lime-slag interface under static experimental conditions as reported in the literature. It is also observed at the lime-slag interface in the slag sample taken from the laboratory hot metal dephosphorisation experiment in an induction furnace in this study. However, this C_2S-C_3P layer is not always observed in the slag samples taken from the 6t pilot plant converter and the 320t industrial converter. The C_2S-C_3P layer observed in Figure 3(c) is more likely to be a layer of precipitated C_2S-C_3P grains surrounded by an FeO/MnO layer. Although the C_2S-C_3P layer might be assimilated by the high FeO/MnO slag, extremely dynamic conditions in the 6t pilot plant converter and 320t industrial converter can be considered as the key for the disappearance of the C_2S-C_3P layer surrounding the lime particles. The boundary layer surrounding the “moving” lime particle with the possibility of the formation of dense C_2S layer can be moved away by the extremely dynamic condition to homogenise the slag composition. This extremely dynamic condition is not available in the laboratory experiments either under static conditions or even in the induction furnace.

As a result of this, it is not certain that the results from static laboratory experiments on the lime dissolution into BOS slag can be fully applicable to the industrial BOS process and the quality of lime assessed at ambient temperature can be linked to the lime dissolution behaviour into slag at steelmaking temperatures. For example, the reactivity of lime assessed with various standards, e.g. measuring the temperature rise of the certain amount of water at designed time, may not be relevant to the reactivity of lime at steelmaking temperature in the BOS process. Therefore, it is necessary to study the dissolution behaviour of lime into slag in a ‘dynamic’ system close to the actual BOS process conditions.

Although no tri-calcium silicate (C_3S) substance / layer was observed at the lime-slag interface in the slag samples taken from the laboratory hot metal dephosphorisation experiment in the induction furnace, C_3S was indeed found in the slag samples taken from the 6t pilot plant converter (Figures 3&4) and the 320t industrial converter (Figure 5). In the 6t pilot plant converter trial (Figure 3), the substances that filled the large cracks / pores are a tri-calcium silicate phase along the channel wall and di-calcium silicate grains in the channel centre surrounded by high FeO/MnO slags. The substances that filled the capillaries of lime particles are mainly a tri-calcium silicate phase. It can be considered that after the slag penetrated into the big cracks / pores and capillaries, the slag has less mobility due to restriction of the space and also the diffusion of Ca^{2+} into the slag and the slag components into the lime, and therefore, after a certain amount of time, C_3S was formed along the channel wall with the right ratio of Ca^{2+} and SiO_4^{4-} (resulted from the continuous diffusion of Ca^{2+}) and the FeO/MnO substance was pushed away from the C_3S layer. In the 320t industrial

converter, C_3S can be considered to be the precipitated product during the slag cooling as the $\%CaO/\%SiO_2$ ratio is high in the slag. Therefore, the formation of C_3S at the lime-slag interface is caused by the restricted slag flow (e.g. under static experimental conditions or in the pores / cracks and small capillaries) and the continuous diffusion of Ca^{2+} into the slag with less mobility.

6. Conclusions

(1) The lime dissolution behaviour into BOS slag was studied by observing the lime-slag interface in the slag samples taken from the laboratory hot metal dephosphorisation experiment in an induction furnace, a 6t pilot plant converter and a 320t industrial converter. Examination of the slag sample from the hot metal dephosphorisation experiment in the induction furnace showed that across the slag-lime particle boundary two layers were detected: a dense and continuous C_2S-C_3P solid solution layer next to the bulk slag and a FeO/MnO-rich layer next to lime. However, no continuous C_2S-C_3P layer was observed for the slag samples taken from the 6t pilot plant converter and the 320t industrial converter.

(2) The dissolution of lime into slag is considered to be two-direction diffusion: outward diffusion of Ca^{2+} into slag and inward diffusion of slag components into lime. The inward diffusion is led by the faster diffusion of the ions of Fe^{2+}, Mn^{2+} and Mg^{2+}, resulting in the formation of an FeO/MnO/MgO-rich layer and followed by the slower diffusion of anion complexes SiO_4^{4+} and PO_4^{3-} resulting in the formation of a C_2S-C_3P solid solution layer.

(3) Early formation of the slag with high Fe^{2+}, Mn^{2+} and Mg^{2+} contents is important to accelerate the dissolution of lime into slag.

(4) The extremely dynamic conditions in the 6t pilot plant converter and the 320t industrial converter removes away the boundary layer surrounding the “moving” lime particle with the possibility of the formation of C_2S layer, which explains the difference in morphology at the lime-slag interface in the slag samples between industrial converter and laboratory static experiment.

(5) It is necessary to study the dissolution behaviour of lime into slag in a ‘dynamic’ system close to the actual BOS process conditions. It is also suggested to check if the result from laboratory static experiments on the dissolution behaviour of lime into BOS slag can be fully applicable to the industrial BOS process and the quality of lime assessed at ambient temperature can be linked to the lime dissolution behaviour into slag at steelmaking temperatures.

(6) The formation of a tri-calcium silicate phase at the lime-slag interface is caused by the restricted slag flow (e.g. under static experimental conditions or in the pores / cracks and small capillaries) and the continuous diffusion of Ca^{2+} into the slag with less mobility.

Acknowledgement

The authors would like to thank Mr G Parker, Mr C Barnes, Mr M Bugdol and Mr C McDonald for their help and support during the investigation.

References

[1] R. O. Russell. Lime reactivity and solution rate. *Journal of Metals*, 1967, p104-106.

[2] B. Deo, K. Gupta, M. Malathi, P. Koopmans, A. Overbosch and R. Boom: Theoretical and practical aspects of dissolution of lime in laboratory experiments and in BOF. T*he 5th European Oxygen Steelmaking Conference* (Aachen, Germany), 2006, p202-209.

[3] J. Yang, M. Kuwabara, T. Asano, A. Chuma and J. Du. Effect of lime particle size on melting behaviour of lime-containing flux. *ISIJ International*, 2007, 47(10), p1401-1408.

[4] T. Deng, J. Gran and D. Sichen: Dissolution of lime in synthetic 'FeO'-SiO_2 and CaO-'FeO'-SiO_2 slags. *Steel Research International*, 2010, 81(5), p347-355.

[5] L. Zhong, K. Mukai, M. Zeze, K. Miyamoto and N. Sano. In-situ Observation of Penetration of Molten Slag into solid Lime at High Temperature. *Steel Research International*, 2007, 78(3), p236-240.

[6] M. Matsushima, S. Yadoomaru, K. Mori and Y.Kawai. A fundamental study of dissolution of solid lime in liquid slag. *Transactions of ISIJ*, 1977, 17, p442-449.

[7] M. Umakoshi, K. Mori and Y. Kawai. Dissolution rate of burnt dolomite in molten FetO-CaO-SiO_2 slags. *Transactions of ISIJ*, 1984, 24(7), p532-539.

[8] J. Pal, S. Ghorai, D. Singh, A. Upadhyay, S. Ghosh, D. Ghosh and D. Bandyopadhyay: Performance assessment of CO_2 treated fluxed iron oxide pellets in basic oxygen steelmaking process. ISIJ International 50(1), 2010. p105-114.

[9] H. Hidetaka. The effect of C_2S saturation on the lime dissolution rate in LD converter. *Tetsu-to-Hagane*, 1980, S760.

[10] T. Hamano, S. Fukagai and F.Tsukihashi: Reaction mechanism between solid CaO and FeO_x-CaO-SiO_2-P_2O_5 slag at 1573K, *ISIJ International*, 2006, 46, p490-495.

[11] X. Yang, R. Saito, T. Hamano, H. Matsuura and F. Tsukihashi. Role of solid CaO in FeO-CaO-SiO_2-P_2O_5 multi-phase flux at hot metal dephosphorisation temperature. *The VIII International Conferences on Molten Slags, Fluxes and Salts (MOLTEN 2009)* (Chile), 2009, p903-911.

[12] M. S. Millman, A. Overbosch, A. Kapilashrami, D. Malmberg and M.Bramming. Study of refining performance in BOS converter. Ironmaking and Steelmaking, 38(7), 2011, p.499-509.

[13] M. S. Millman, A. Overbosch, A. Kapilashrami, D. Malmberg and M.Bramming. Sampling the slag/metal emulsion in a BOS converter-Phosphorus control. *The 3rd international conference on process development in iron and steelmaking (SCANMET III)* (MEFOS, Sweden), 2008.

[14] S. Kitamura, H. Shibata, K. Shimauchi and S. Saito. Importance of dicalcium silicate for hot metal dephosphorisation reaction. *La Revue de Metallurgie*, 2008, p263-271.

[15] VDEh. *SLAG ATLAS*, 1995, p139.